ELSEVIER

Journal of Hazardous Materials B133 (2006) 276–282

Journal of Hazardous Materials

www.elsevier.com/locate/jhazmat

Surface modification of purified fly ash and application in polymer

Yang Yu-Fen [a,b], Gai Guo-Sheng [a,*], Cai Zhen-Fang [a], Chen Qing-Ru [b]

[a] *Powder Technology R & D Group, Department of Materials Science and Engineering, Tsinghua University, Beijing 100084, China*
[b] *School of Chemistry and Environmental Engineering, China University of Mining and Technology, Beijing 100083, China*

Received 30 May 2005; received in revised form 10 October 2005; accepted 17 October 2005
Available online 28 November 2005

Abstract

With the growing general concern about the pollution by fly ash (FA), there has been global interest in its utilization. Purified FA or FA micro-beads are suitable as polymer filling materials because of their density, good dispersity and fluidity of globular particles. However, FA as a filler has not been widely used up to now on account of low whiteness values and low friction of untreated FA surface. In order to improve the FA quality, a surface modification method by using isothermal heating is proposed in this paper. Preparation of composite fly ash (CFA) in the $Ca(OH)_2$–H_2O–CO_2 system is described. Good coating results on FA surfaces can be achieved under suitable operating parameters. The characteristics of CFA are discussed and analyzed based on data from X-ray diffraction, scanning electron microscopy (SEM), infrared spectra, and BET multiple-point nitrogen adsorption method. Feedstocks with less than 45 μm grain size, 2.86 $m^2\,g^{-1}$ specific surface area, and 36.68 whiteness value revealed an increase in specific surface area ranging from 8.69 to 10.01 $m^2\,g^{-1}$ and an increase in whiteness values ranging from 63.67 to 73.13 after coating. A SEM study allowed a detailed determination of the morphology of the surface roughness. Filling tests also show that a rough surface of the CFA enhances contact opportunities and improves the interface between polymer and CFA blended with polypropylene (PP).

Keywords: Fly ash; Surface modification; Composite fly ash; Filling; Polymer

1. Introduction

In order to reduce the production cost of plastic products, and to improve certain characteristics, one or more filler is usually used as an addition to the resin matrix. Purified fly ash (FA) containing 90% globular particles with a reasonable size distribution, low density, good shape with good dispersity and fluidity is suitable as a polymer filling material [1,2]. Alkan et al. studied on production of a new material from fly ash and polyethylene [3]. Zheng studied changes in the mechanical properties of the composite system of PP-FA after DL-411-DF ingredients as coupling agents were added [4]. Ma studied superfine fly ash considering different coupling agents and showed that a mixture with noumenon polypropylene powder can be developed into a special material for use in middle-price pipe material [5].

However, the use of FA as a filler is still not widespread. The main reasons are the weak interfacial bonding between untreated FA and polymer due to the low friction of the FA surface, and the low whiteness value resulting in an undesirable appearance to the final product. Several common surface modification technologies, involving addition of either coupling-agents or surfactants followed by mechanical mixing, have been widely used to modify the surface properties of FA [4,5]. These chemical modification methods can improve to a certain degree the interfacial properties between FA and a polymer. Changes in the surface morphology and the surface area of fly ashes with solutions of NaOH, $NaOH/NH_4HCO_3$, EDTA, and HCl have been reported [6]. However, the disposal of alkaline or acidic wastewater presents an additional difficulty. Additionally, these methods cannot improve the color, restricting the wide use of FA as a filler. In order to meet the demands of the plastics industry for fillers with high quality, developing a surface modification technology [7–9] to improve FA properties with high whiteness values and large specific surface area is an important research keystone.

The purpose of this paper is to investigate these problems associated with utilization of purified FA as a filler in polymers. CFA as a filler appears to be suitable, however, till now, there has

* Corresponding author. Tel.: +86 10 6278 1144; fax: +86 10 6279 1258.
E-mail address: gaigs@mail.tsinghua.edu.cn (G.-S. Gai).

0304-3894/$ – see front matter © 2005 Elsevier B.V. All rights reserved.
doi:10.1016/j.jhazmat.2005.10.028

been no report of using the isothermal heating method to modify and prepare CFA with high whiteness value and large specific surface area. The emissions of FA amounted to 190.8 million tonnes in 2003 and 228 million tonnes in 2004 in coal-fuelled power stations in China. The utilization ratio was however only 55.8% in 2003 and 55.7 wt% in 2004 [10,11]. Research work into improved utilization of FA is therefore of practical significance.

2. Experiments

2.1. Analytical methods

A scanning electron microscope (SEM), CSM-950 (OPTON, Germany), was used to observe the surface morphology of FA before and after coating. Phase identification was performed by X-ray diffraction analysis using a D/max-RB X-ray diffractometer (Japan Science Company). The specific surface area was determined from the nitrogen adsorption data by the BET method, using a NOVA4000 high-speed automatic surface area analyzer. Fourier transform infrared spectroscopy (FTIR) (Nicolet560, USA), was used to mensurate the changes in OH and Si–O–Si groups between FA and CFA. Whiteness values were mensurated using a ZBD type whiteness-meter produced by Wenzhou Ludong Apparatus Factory of Zhejiang Province. The mechanical properties of PP-based composites were examined by several methods including a Ø 30 × 45 twin screw extruder (W & P, Germany), an injection-moulding machine (150ZP, Hongkong Zhenxiong Machinery Co., Ltd.), a RTM-250 type electron tensile testing systems from Instron America, and a XJZ-50 type impacting tester (Chengteh Testing Machine Co., Ltd., China).

2.2. Preparation of purified FA

Original wet-collected FA samples were sampled from Huaneng Dezhou Power Plant of Shandong Province. The chemical composition consisted of 54.69 wt% SiO_2, 33.50 wt% Al_2O_3, 3.00 wt% CaO, 0.98 wt% MgO, 6.73 wt% Fe_2O_3, 0.36 wt% K_2O and 0.74 wt% TiO_2, in which SiO_2 and Al_2O_3 accounted for nearly 90%. The true density was 2.18 g/cm^3. The unburned carbon content was 8.25 wt%.

The FA sample was first classified with a 45 μm wet classifier to obtain sample A with less than 45 μm grain size. A magnetic separator with 7000-G magnetic induction intensity was used to separate the magnetic fraction from sample A to get sample B, and then a small XFD-type flotator was used to remove unburned carbon from the sample B to obtain sample C. The chemical composition of sample C included 57.94 wt% SiO_2, 34.97 wt% Al_2O_3, 2.84 wt% CaO, 0.91 wt% MgO, 1.78 wt% Fe_2O_3, 0.65 wt% K_2O and 0.91 wt% TiO_2. The true density was 1.99 g/cm^3. The unburned carbon content was reduced to 0.45 wt%. Hereafter we refer to sample C as purified FA.

2.3. Preparation of CFA

The FA surface modification experiments were performed in an open vessel with a stirrer at normal pressure and below 100 °C. Two thousand milliliters mixing slurry including $Ca(OH)_2$ solution, and sample C together with tap water were put into the vessel, which was placed on an electric cooker. $Ca(OH)_2$ solution was obtained by slaking lime-stone supplied by Beijing Fangshan lime factory. The FA/$Ca(OH)_2$ weight ratio was 5:1. The water/solid weight ratios (L/S) tested were 5–20:1. The slurry was fully agitated by the stirrer at 350–450 rpm and fleetly heated up to 80–95 °C and then isothermally heated for 0.5–7 h. The temperature was kept constant by a temperature regulation meter.

For SEM, XRD, FTIR, and BET analyses, only a little amount of sample was needed. During the isothermal heating, at the required heating time, a sample of each was directly scooped from the slurry. These samples were filtered and the residues left were dried at 110 °C in an oven for several hours till they were fully dried. The dried cakes were crushed into powders which were cased in individual valve bags.

For whiteness value and filling performance test samples, at the stated heating times, the electric cooker was turned off and then the slurry was cooled to 25–35 °C. After cooling, CO_2 gas was passed through the vessel to neutralize the redundant $Ca(OH)_2$ in order to obtain neutral filler. This carbonization process usually lasted 20–30 min. The pure CO_2 gas used in the experiment was bought from a standard commercial source. Slurry-circulation and continuous-stirring were needed to boost the reaction between CO_2 and $Ca(OH)_2$. The circulating volume was 60 l/min. The pH value was measured on-line with a pH meter, which was standardized before and after each experiment with standard buffer solutions. The reaction was judged to be completed when the pH value of the slurry reached 7. After the reaction was completed, the slurry was filtered and the solid material was dried using the oven.

3. Results and discussion

3.1. Surface morphology of particles

In order to obtain high added-value CFA with higher whiteness and larger specific surface area, several parameters must be effectively controlled and adjusted during the reaction. For production of CFA, the conditions used were FA/$Ca(OH)_2$ weight ratio of 5:1, water/solid ratio of 20:1, 95 °C slurry temperature, 360 rpm stirring speed and 4 h isothermal heating. SEM photomicrographs showing the surface morphology of the FA before and after coating are given in Fig. 1. It can be seen from Fig. 1a that nearly 100% of the particles are globular or elliptoid with smooth surface and good dispersity. Compared with the uncoated FA, the CFA particles (Fig. 1b) possess a rough surface: the uncoated FA smooth surface caused by sharply cooling after high temperature fusing has thus been transformed. A large number of small granular particles are attached to the surface of the CFA. The particles coated onto the surface of the FA particles have sizes of less than 1 μm. Similar SEM photomicrographs were obtained for 5, 6 or 7 h isothermal heating. The surface modification method has good reproducibility and low cost.

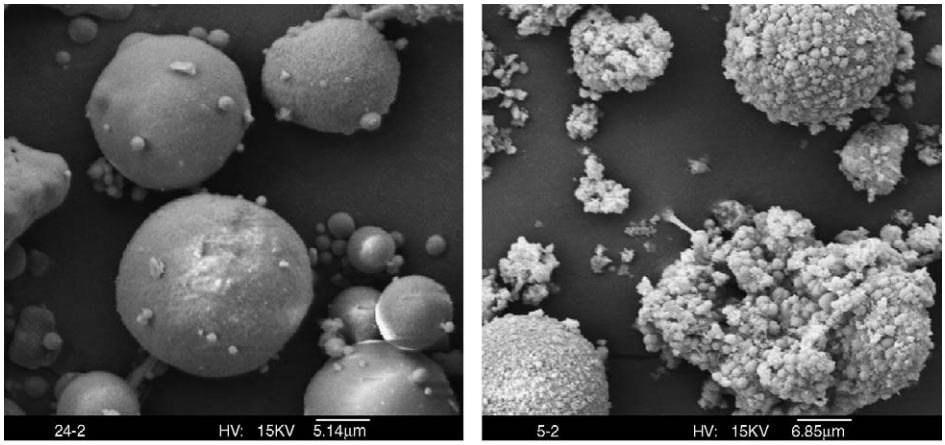

Fig. 1. SEM photographs of surface morphology of FA and CFA. (a) Surface morphology of FA and (b) surface morphology of CFA.

3.2. Specific surface area

The BET method was used to measure the specific surface area of FA and CFA. The results, given in Table 1, show that the specific surface area of CFA is three times greater than that of the FA. This is mainly attributed to the changes in surface morphology and the formation of the rough surface of CFA. This indicates that the coating particles on the FA give rise to a substantial increase in the CFA specific surface area. Compared to FA, CFA can be expected to have a better contact interface with a polymer matrix when CFA is used as the polymer filling material, on account of the larger specific surface area and the rough surface. The operating conditions used were FA/$Ca(OH)_2$ weight ratio of 5:1, water/solid ratio of 7:1, 95 °C slurry temperature, 400 rpm stirring speed and 4 h isothermal heating.

3.3. XRD analyses

X-ray diffraction (XRD) was employed to analyze the crystal structure and orientation. The XRD pattern of purified FA (Fig. 2) shows the existence of mullite (card no. 150776; 3.397, 3.429, 2.210, and 5.395 Å), quartz (card no. 650466; 3.353, 4.26, and 1.844 Å) and a small amount of hematite (card no. 240072; 2.698, 2.52, and 1.702 Å). The characteristic peaks of mullite are strong and correspond to crystallization. Mullite, formed by SiO_2 reacting with Al_2O_3 at high temperature of 1200–1650 °C in a boiler of the power plant, has very stable crystalline structure. The X-ray diffraction pattern also shows a mild hump ranging from 20° to 25°, characterizing the existence of amorphous alumina and silica with higher activity [12,13]. The fly ash contains both quartz and amorphous silica. The amorphous silica is more active than the crystalline quartz. The former predominates in participating in the pozzolanic reaction.

The XRD pattern of CFA (Fig. 3) shows that significant changes in the intensities of the characteristic peaks. The operating conditions used were FA/$Ca(OH)_2$ weight ratio of 5:1, water/solid ratio of 7:1, 90 °C slurry temperature, 400 rpm stirring speed and the sampling times are 0.5, 1, 2, 3, 4, 5, 6, and 7 h.

It can be seen from Fig. 3 that with increasing heating time the characteristic peaks of $Ca(OH)_2$ become weaker, whereas the characteristic peaks of silicate and aluminate products become stronger, indicating that more $Ca(OH)_2$ is consumed and more silicate and aluminate compositions is formed. Various silicate and aluminate components with different molecular formulas and characteristic peaks coexistent in the system, these are listed in Table 2.

Untreated FA itself is of lower activity [14]. The glassy surface layer of the FA particles is dense and chemically stable. This layer protects the inside constituents, which are porous, spongy, and amorphous, and therefore have higher activity. The silica–alumina glassy chain of high Si, Al and low Ca content is stable; the chain must be disintegrated to promote chemical activity. On account of the $Ca(OH)_2$ solution with higher

Table 1
Specific surface area of FA and CFA

Samples	Specific surface area ($m^2\ g^{-1}$)
Sample C	2.86
Sample F	8.69–10.01

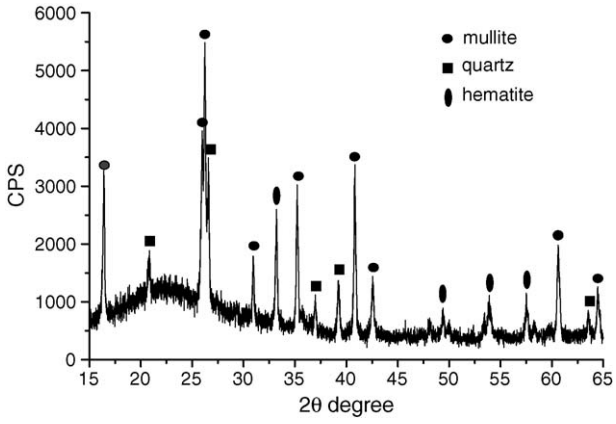

Fig. 2. X-ray diffraction pattern of sample C.

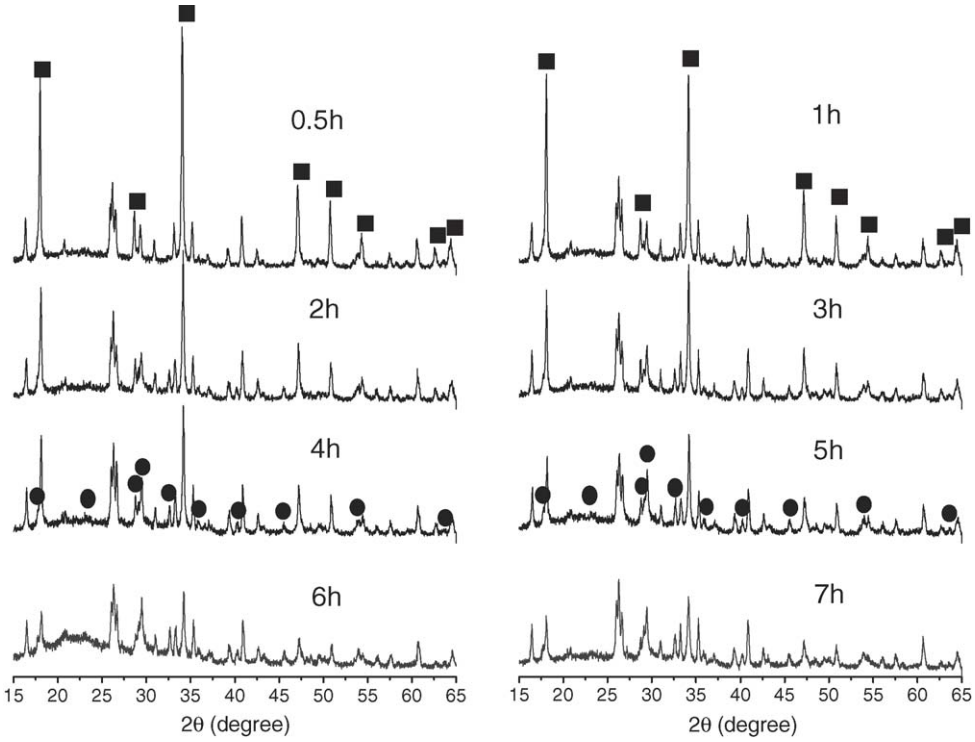

Fig. 3. XRD patterns of CFA after isothermal heating. (■) $Ca(OH)_2$, and (●) silicate and aluminate compositions.

basicity, the densified outer layer is corroded and the active core is exposed [15]. If the OH^- concentration is high enough, the silica–alumina glassy chain will be rapidly disintegrated and will produce a large number of active groups. With the corrosion of the outer glassy surface layer, the inside active constituents are also dissolved [16]. On account of the chemically activated FA, the active silica and alumina react with hydrated lime to form varieties of silicate, and aluminate products, which deposit, nucleate and grow on the FA particle surfaces. These reactants coated on the FA particle surfaces not only alter the surface morphology of CFA but also enhance the whiteness value of CFA.

3.4. FTIR analyses

3.4.1. Influence of isothermal heating time on –OH group

FTIR spectra ranging from 4000 to 2800 cm^{-1} of the purified FA and three CFA samples of 2, 4, or 6 h isothermal heating are presented in Fig. 4. The technological conditions include: 90 °C slurry temperature, 360 rpm agitating speed, L/S = 10:1, and FA/$Ca(OH)_2$ weight ratio of 5.

The FTIR spectrum of purified FA without the characteristic 3400 cm^{-1} bands for stretching vibration of the OH group is different to that of the CFA. The results show that there are some components with an –OH group or crystal lattice water

Table 2
The molecular formula and their characteristic peaks for silicate and aluminate products

No.	Molecular formula	Card no.	Heating time (h)	Characteristic peaks (Å)
1	Ca_2SiO_4	231045	0.5, 1	2.886[a], 2.749, 1.993
2	$Ca_2SiO_4{\cdot}3H_2O$	290374	0.5, 1, 2	3.110[a], 3.072, 2.886
3	$Ca_6Si_3O_{12}{\cdot}H_2O$	140035	1, 2, 3	3.429, 3.072, 2.293[a]
4	$Ca_3Al_6Si_2O_{16}$	230105	1, 2, 3	3.035, 2.98[a], 2.886
5	$CaAl_2Si_4O_{12}{\cdot}2H_2O$	421451	3, 4, 5	5.604, 3.390[a], 2.884
6	$CaAl_2(SiO_3)_4{\cdot}2H_2O$	421451	3, 4, 5	5.604, 3.390[a], 2.884
7	$Ca_3Al_2\ (SiO_4)_3$	390368	4, 5, 6	2.956, 2.65[a], 1.579
8	$Ca_3Al_2(SiO_4)(OH)_8$	320151	4, 5, 6	2.741[a], 2.240, 1.990
9	$Ca_3Al_2(SiO_4)_{1.25}(OH)_7$	451447	4, 5, 6	2.741[a], 2.240, 1.990
10	$CaAl_2Si_2O_7(OH)_2H_2O$	130533	4, 5, 6	2.73, 2.621[a], 1.55
11	$Ca_3Si_3O_9H_2O$	290378	4, 5, 6	3.20[a], 3.03, 2.93
12	$Ca_2Al_3\ (SiO_4)(Si_2O_7)(O,OH)$	441400	5, 6	3.474, 3.064, 2.884[a]
13	$Ca_2Al_3\ (SiO_4)(Si_2O_7)(O,OH)_2$	130562	5, 6	4.03, 2.884, 2.695[a]
14	$Ca_5Al_5O_{14}$	110357	5, 6	2.93[a], 2.884, 2.487

[a] Strongest.

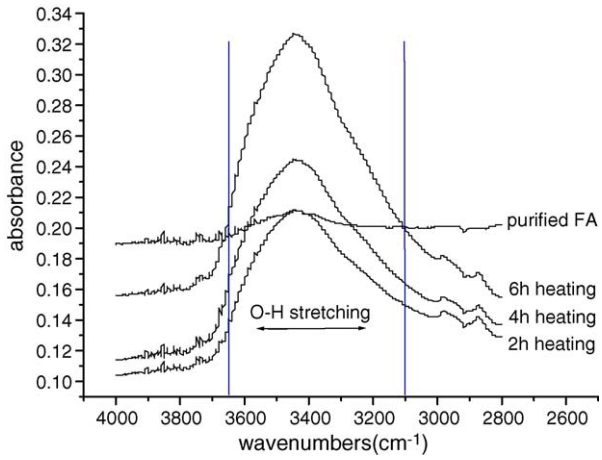

Fig. 4. FTIR spectra ranging from 4000 to 2800 cm^{-1} of the four samples.

coated on the surface of CFA, as was also indicated by the XRD analyses. This conclusion is based on observations of the –OH and H_2O symmetric stretching between 3650 and 3100 cm^{-1} in Fig. 4. The three CFA samples for 2, 4 or 6 h isothermal heating exhibit considerable differences in the percentage of –OH groups. This indicates that the percentage of –OH groups increases with isothermal heating time [17,18].

3.4.2. *Influence of isothermal heating time on Si–O–Si group*

The changes of FTIR spectra ranging from 1400 to 900 cm^{-1} of the four samples are presented in Fig. 5. The FTIR peak at 1085 cm^{-1} for the purified FA sample corresponds to the internal SiO_4 tetrahedra, especially the Si–O–Si chain structure (Fig. 5). The peaks at 1010–1090 cm^{-1} of the CFA samples correspond to a cyclic Si–O–Si structure. This means that the random glass network of the untreated FA changed into a zeolite-like structure with an heating time.

For stretching vibration of the Si–O–Si group, it can be seen from Fig. 5 that there is an excursion [19,20] between the spectrum of purified FA and that of the CFA. The excursion becomes wider with the increasing heating time. The results indicate that silicate products have various chemical structures. These components include $Ca_2SiO_4{\cdot}3H_2O$ (card no. 290374) with single-silicic acid radical, $CaAl_2Si_2O_7(OH)_2{\cdot}H_2O$ (card no. 130533) with two-silicic acid radical, $Ca_3Si_3O_9{\cdot}H_2O$ (card no. 290378) with three-silicic acid radical, $CaAl_2Si_4O_{12}{\cdot}2H_2O/CaAl_2(SiO_3)_4{\cdot}2H_2O$ (card no. 421451) with quad-silicic acid radical, and so on.

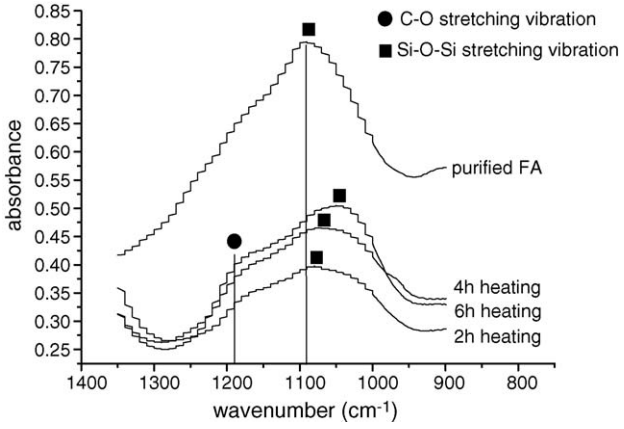

Fig. 5. FTIR spectra ranging from 1400 to 900 cm^{-1} of the four samples.

In addition, another absorption peak at about 1200 cm^{-1} can be seen in Fig. 5 that this peak corresponds to the C–O stretching vibration, which suggests that carbonates, such as $CaCO_3$, remain after the isothermal treatment. This can be understood as $CaCO_3$ is very easily formed on the surface of bulk solution in the open vessel because of the high reaction equilibrium constant 2.312×10^8 for the equation $Ca(OH)_2 + CO_2 \rightarrow CaCO_3 + H_2O$ [21].

3.5. *Whiteness analyses*

The codes and whiteness values (dimensionless) for the different samples are listed in Table 3. CFA (referred to as sample F) was prepared using sample C as a feedstock. One can see from Table 3 that the whiteness value of sample C is only 36.68. After 5 h isothermal heating as well as 20–30 min carbonization, the whiteness value of sample F can be enhanced to the range from 63.67 to 73.13. The other important operating conditions used were 95 °C slurry temperature, 400 rpm stirring speed, FA/$Ca(OH)_2$ weight ratio of 5:1, water/solid ratios of 5:1, 7:1, 10:1, 15:1, and 20:1, respectively. The whiteness value of CFA is therefore increased by 73.58–99.37% compared to that of the untreated FA. The color difference between sample C and sample F is so obvious that it can be observed by a naked eye. A comparison of the appearance of the different samples is shown in Fig. 6. The appearance of sample F was greatly altered by the treatment.

Unburned carbon particles usually are of relatively large size and mainly concentrate in the fraction of +45 μm grain size. The content in sample A is only 2.61%. It can be seen from Fig. 6 that although the content is lower, the ultra-fine unburned carbon (sample D) presents a dark-grey and black appearance with a whiteness value of only 22.29. There is therefore a need to remove these particles before the modification procedure. The unburned carbon particles can be easily removed from fly ash by a froth flotation method [22] because they are not conglomerated in the materials. The removal rate of unburned carbon can be up to 98% by the small-type flotation separator used in our lab. Some experiments were conducted in order to examine influ-

Table 3
Code and whiteness value of different samples

Sample code	Whiteness
Sample A: FA with less than 45 μm grain size	29.8
Sample B: FA after removing magnetic pearls	33.54
Sample C: FA after removing magnetic pearls and unburned carbon	36.68
Sample D: Unburned carbon	22.29
Sample E: Magnetic pearls	9.5
Sample F: CFA	63.67–73.13

Fig. 6. Comparison of the appearance of the different samples.

ence of unburned carbon on the whiteness value of CFA. Using sample C as feedstock, the whiteness values for CFA can be up to the range from 63.03 to 73.13. Using sample B as feedstock, the highest whiteness value for CFA is only 60.93. Therefore, removal of unburned carbon is very important to enhance the quality of the final CFA.

The composition of magnetic pearls with strong magnetic properties [23] are Fe_3O_4 and Fe_2O_3. These are formed by decomposing pyrite, magnetite and other minerals during coal combustion. It can be seen from Fig. 6 that the magnetic pearls (sample E) with only 9.5 whiteness value result in a black appearance and have a very strong influence on the whiteness value of sample A. However, 93% the magnetic pearls can be removed from sample A by the small-type magnetic separator used in our lab.

4. Filling test

To compare their filling properties, FA and CFA were used to produce different compound polypropylene (PP) materials with a 25% filling ratio by our partner, the Chinese Institute of Plastics Processing and Application of Light Industry as a cooperative effort toward practical applications. The PP was sourced from the Sinkiang Dushanzi Petrifaction Corporation. The procedure for preparation of the FA/PP or CFA/PP composites is as follows. Further details are given elsewhere [24]. (1) The FA or CFA powders were organically treated for 15 min by a high speed mixer at the temperature range from 100 to 120 °C using XH–CR11 surfactant, purchased by Nanjing Consonancy Chemical Ltd. Company. (2) The above powders cooled were mixed with pure PP using the two-roll mill at the room temperature. (3) The mixing-powders of FA/PP or CFA/PP were compounded using the twin-screw extruder at 180–210 °C, and the pelletizer used to produce composite FA/PP or CFA/PP pellets. The rotation speed of the extruder was set to 200 rpm. (4) These resultant pellets were moulded into either impact-test-samples according to the Chinese National Standard GB1043-93 or the tensile-test-samples (Standard GB1040-92) with the injection-moulding machine at 210 °C. (5) Tensile testing of the composites was conducted using an electronic tensile testing system, and impact testing was conducted using an impacting tester. Five samples were tested for each case. For sake of comparison, a similar procedure was used to prepare blank nofiller PP materials.

The mechanical testing results of FA/PP and CFA/PP composites are shown in Table 4. SEM photomicrographs showing the fracture surfaces of PP, FA/PP and CFA/PP broken at low temperature cooled by liquid nitrogen are shown in Fig. 7.

It can be seen from Table 4 that although the impact strength of the CFA/PP composites is inferior to that of the pure PP material, the mechanical performance of the CFA/PP composites is obviously superior to that of the FA/PP composites. For the CFA/PP composites, the impact strength, fracture strength and tensile strength are increased by 46.51, 21.37, and 14.65%, respectively, compared to those of the FA/PP composites. One

Table 4
Mechanical properties of composite PP materials (MPa)

Samples	Tensile strength	Fracture strength	Impact strength (10 kJ/m^2)	Elastic modulus	Yield strength
Pure PP	18.6	15.1	19.3	417.7	18.6
FA/PP	15.7	13.1	4.3	394.4	15.7
CFA/PP	18.0	15.9	6.3	430.1	18.0

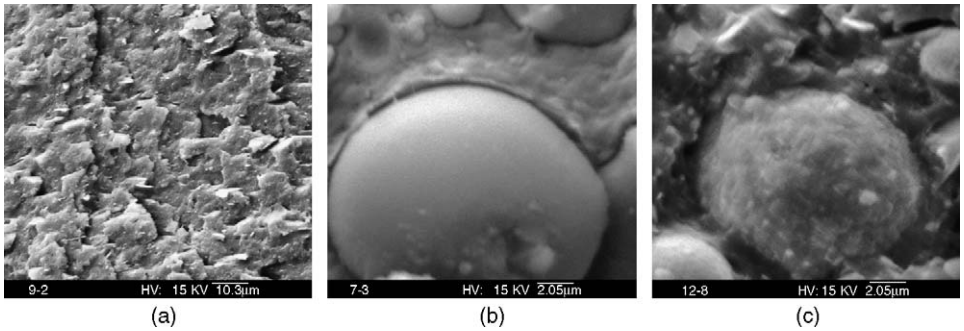

Fig. 7. SEM photomicrographs of composites PP fracture surface. (a) Pure PP, (b) FA/PP, and (c) CFA/PP.

can distinctly see from Fig. 7c that there is close bonding and better consistency between the CFA and the PP matrix. In contrast, some weak links and obvious grooves and gaps exist between the FA particles and the PP matrix (Fig. 7b). The matching effect of CFA as filler in PP is therefore better than that of FA as filler in the same PP. This improvement can mainly be attributed to the changes in the surface morphology of CFA. The coating of silicate and aluminate reactants on the CFA surface allows the formation of a rough surface with a larger specific surface area. This increases contact opportunities between the CFA and polymer, and improves the interfacial properties between them when CFA is blended with a PP polymer.

5. Conclusions

(1) Due to the addition of a $Ca(OH)_2$ solution with high basicity, the densified outer layer of FA is corroded at the beginning of processing. A large number of porous, spongy, amorphous constituents with higher activity than in untreated samples are produced.
(2) On account of the chemically activated FA, the active silica and alumina react with hydrated lime to form a variety of silicate and aluminate reactants which deposit, nucleate and grow on FA particle surface to form CFA particles with rough surfaces and large specific surface areas. CFA prepared in the $Ca(OH)_2$–H_2O–CO_2 system has a high whiteness value and good appearance. These experiments are of good reproducibility.
(3) The mechanical performance of the CFA/PP composite is superior to that of the FA/PP composites. This is attributed to the surface roughness of CFA, which increases contact opportunities between the CFA and polymer matrix and improves the interfacial properties between them when they are blended.

Acknowledgements

The financial support provided for the project (project number 50474003) by the National Natural Science Foundation of China is gratefully acknowledged. The authors would also like give special thanks to Prof. A. Godfrey for assistance with proofreading of the text.

References

[1] S. Horiuchi, M. Kawaguchi, K. Yasuhara, Effective use of fly ash slurry as fill material, J. Hazard. Mater. 76 (2–3) (2000) 301–333.
[2] H.F. Yang, Q. Zhang, Reuse and Recycle of Solid Waste, Chemical Industry Press, Beijing, 2003, 165.
[3] C. Alkan, M. Arslan, M. Cici, M. Kaya, M. Aksoy, A study on the production of a new material from fly ash and polyethylene, Resour. Conserv. Recycl. 139 (3–4) (1995) 147–154.
[4] Y.Y. Zheng, Application of powder coal ash glass-microballons to polypropylene plastics, J. Fuzhou Univ. (Nat. Sci.) 26 (2) (1998) 87–90.
[5] J. Ma, The development of special polypropylene filled with superfine fly ash, Fly Ash Compr. Util. (4) (2001) 17–20.
[6] Z. Sarbak, M. Kramer-Wachowiak, Porous structure of waste fly ashes and their chemical modifications, Powder Technol. 123 (1) (2002) 53–58.
[7] G.S. Gai, Y.F. Yang, S.M. FAN, Preparation and properties of composite mineral powders, Powder Technol. 153 (3) (2005) 153–158.
[8] S.M. Fan, Y.F. Yang, G.S. Gai, H.Z. Miao, Preparation of composite wollastonite powder with nano-structure surface, Rare Metal Mater. Eng. 32 (Suppl. 1) (2003) 702–704.
[9] S.M. Fan, Y.F. Yang, G.S. Gai, H.Z. Miao, Research on dolomite powder with nanometer surface structure, Rare Metal Mater. Eng. 32 (Suppl. 1) (2003) 805–807.
[10] State Environmental Protection Administration of China, Report on the State of the Environment in China 2003, China Environment News, June 3, 2004.
[11] State Environmental Protection Administration of China, Report on the State of the Environment in China 2004, China Environment News, June 10, 2005.
[12] R.B. Lin, S.M. Shih, Characterization of $Ca(OH)_2$/fly ash sorbents for flue gas desulfurization, Powder Technol. 131 (2–3) (2003) 212–222.
[13] R.B. Lin, S.M. Shih, C.F. Liu, Characteristics and reactivities of $Ca(OH)_2$/silica fume sorbents for low-temperature flue gas desulfurization, Chem. Eng. Sci. 58 (16) (2003) 3659–3668.
[14] Y.M. Fan, S.H. Yin, Z.Y. Wen, J.Y. Zhong, Activation of fly ash and its effects on cement properties, Cem. Concr. Res. 29 (1999) 467–472.
[15] S. Yan, A.L. Cai, F.X. Yu, C.H. Jaing, Dissolving mechanism of high calcium high sulfate fly ash in water, J. Nanjing Univ. Technol. 25 (3) (2003) 17–22.
[16] S. Goñi, A. Guerrero, M.P. Luxán, A. Macías, Activation of the fly ash pozzolanic reaction by hydrothermal conditions, Cem. Concr. Res. 33 (9) (2003) 1399–1405.
[17] O.E. Omotoso, D.G. Ivey, R. Mikula, Characterization of chromium doped tricalcium silicate using SEM/EDS, XRD and FTIR, J. Hazard. Mater. 42 (1) (1995) 87–102.
[18] L.J. Neergaard, M.B. Nawaz, Dry-pressing behavior of silicone-coated alumina powders, Powder Technol. 98 (2) (1998) 104–108.
[19] Y.Q. Wang, X.B. Liao, H.W. Diao, Tiny structure of hydrogenation amorphous silicon films, Sci. China (Series A) 32 (6) (2002) 531–537.
[20] Y.Q. Lu, Z.H. Deng, Practical Infrared Spectrum Analyses, first ed., Electron Industry Press, Beijing, 1989, 99-104, 143-146, 176-179.
[21] Q.F. Hu, X.B. Hu, B.X. Liu, New combination carbonation technique of producing nanosize calcium carbonate, Non Metal. Mines 27 (6) (2004) 30–33, 55.
[22] M.L. Gray, K.J. Champagne, Y. Soong, R.P. Killmeyer, M.M. Maroto-Valer, Physical cleaning of high carbon fly ash, Fuel Process. Technol. 76 (1) (2002) 11–21.
[23] S. Prakash, J.K. Mohanty, B. Das, R. Venugopal, Characterisation and removal of iron from fly ash of Talcher Area, Orissa, India, Miner. Eng. 14 (1) (2001) 123–126.
[24] C.L. Wu, M.Q. Zhang, M.Z. Rong, K. Friedrich, Tensile performance improvement of low nanoparticles filled-polypropylene composites, Compos. Sci. Technol. 62 (10–11) (2002) 1327–1340.